

Article

Tuning the Latency by Anionic Ligand Exchange in Ruthenium Benzylidene Phosphite Complexes

Nebal Alassad¹, Ravindra S. Phatake^{1,2,*} , Mark Baranov¹ , Ofer Reany^{1,3}  and N. Gabriel Lemcoff^{1,4,*} 

¹ Chemistry Department, Ben-Gurion University of the Negev, Beer-Sheva 8410501, Israel; nebala@post.bgu.ac.il (N.A.); markbara@post.bgu.ac.il (M.B.); offerre@openu.ac.il (O.R.)

² Natural Products and Medicinal Chemistry Division, CSIR-Indian Institute of Integrative Medicine, Jammu 180001, India

³ Department of Natural Sciences, The Open University of Israel, Ra'anana 4353701, Israel

⁴ Ilse Katz Institute for Nanoscale Science and Technology, Beer-Sheva 8410501, Israel

* Correspondence: ravindra.phatake@iiim.res.in (R.S.P.); lemcoff@bgu.ac.il (N.G.L.)

Abstract: Recently discovered *cis*-dichloro benzylidene phosphite complexes are latent catalysts at room temperature and exhibit exceptional thermal and photochemical activation behavior in olefin metathesis reactions. Most importantly, the study of these catalysts has allowed their introduction in efficient 3-D printing applications of ring-opening metathesis derived polymers and the control of chromatically orthogonal chemical processes. Moreover, their combination with plasmonic Au-nanoparticles has given rise to novel smart materials that are responsive to light. Given the importance of the ligand shell in the initiation and reactivity behavior of this family of complexes, we set out to investigate the effect of anionic ligand exchange. Thus, we report herein two new ruthenium benzylidene benzylphosphite complexes where the chloride anionic ligands have been replaced by bromide and iodide anions (*cis*-Ru-Phos-Br₂ & *cis*-Ru-Phos-I₂). The thermal and photochemical activations of these dormant catalysts in a variety of ring-closing and ring-opening metathesis polymerization (RCM and ROMP) reactions were thoroughly studied and compared with the previously known chloride precatalyst. Photochemical RCM studies provided similar results, especially in non-hindered reactions, with the UV-A wavelength being the best in all cases. On the other hand, the thermal activation profile exposed that the anionic ligand significantly affects reactivity. Notably, *cis*-Ru-Phos-I₂ disclosed particularly impressive initiation efficiency compared to the other members of the family.

Keywords: olefin metathesis; Ru-phosphite complexes; anionic ligands; reaction kinetics



Citation: Alassad, N.; Phatake, R.S.; Baranov, M.; Reany, O.; Lemcoff, N.G. Tuning the Latency by Anionic Ligand Exchange in Ruthenium Benzylidene Phosphite Complexes. *Catalysts* **2023**, *13*, 1411. <https://doi.org/10.3390/catal13111411>

Academic Editor: Tomasz K. Olszewski

Received: 7 October 2023

Revised: 29 October 2023

Accepted: 31 October 2023

Published: 2 November 2023



Copyright: © 2023 by the authors. Licensee MDPI, Basel, Switzerland. This article is an open access article distributed under the terms and conditions of the Creative Commons Attribution (CC BY) license (<https://creativecommons.org/licenses/by/4.0/>).

1. Introduction

The development of ruthenium-based olefin metathesis catalysts has undoubtedly revolutionized the field of organic synthesis over the past few decades [1–3]. Ruthenium catalysts offer exceptional activity, stability, and versatility, enabling the efficient formation and rearrangement of carbon–carbon double bonds in various olefin substrates [1–5]. Their evolution from early generation catalysts to highly efficient and selective species has played a pivotal role in advancing the synthesis of complex molecules, including pharmaceuticals, dyes, materials, and natural products [4–9]. This progress has not only greatly expanded the synthetic chemist's toolbox but has also significantly impacted industries, fostering innovation and sustainability in chemical processes. Although ruthenium olefin metathesis catalysts have been intensively studied and are known for their excellent reactivity, this research field is quite popular, mainly because it offers a reliable, adaptable synthetic tool for both commercial and academic applications and because there are still challenges to be met, both in the selectivity and longevity of the catalysts. Accordingly, the efficiency and selectivity of ruthenium catalysts for olefin metathesis processes have been significantly improved by fine-tuning the ruthenium framework (ligand sphere) [10–12]. Among these,

ruthenium phosphite complexes have received much interest due to their high activity and stability [13–18]. Phosphite ligands in ruthenium phosphite complexes can modify the reactivity and selectivity of the catalyst, making them particularly interesting for olefin metathesis. These complexes have been explored for their ability to promote various types of olefin metathesis reactions, including ring-closing metathesis (RCM), cross-metathesis (CM), ring-opening metathesis polymerization (ROMP), acyclic diene metathesis polymerization (ADMET), and enyne metathesis, among others. The choice of the specific phosphite ligand and its steric and electronic properties can influence the efficiency and scope of these metathesis reactions. The Cazin group pioneered the indenylidene-type phosphite-containing ruthenium complexes (*cis*-Caz-1; Umicore M22), which demonstrated an unusual *cis*-dichloro structural arrangement, room temperature latency with thermal activation, and greatly improved activity at low catalyst loadings (Figure 1) [14]. Later, it was found that UV-A light irradiation of *cis*-Caz-1 catalyzes olefin metathesis reactions (RCM, CM, and ROMP) at ambient temperatures [15]. Moreover, adding a chelating phosphite ligand afforded the highly latent precatalyst *cis*-PhosRu-1 (Figure 1). Surprisingly, the non-chelated benzylidene phosphite complexes were found in the active (non-latent) *trans*-dichloro geometries (*trans*-Ru-P(OEt)₃ & *trans*-Ru-P(O^{*i*}Pr)₃) and catalyzed olefin metathesis reactions at ambient temperatures (Figure 1) [15]. Notably, introducing benzyl phosphite ligands allowed for the design of the *cis*-dichloro complexes *cis*-Ru-1 and *cis*-Ru-2 (Figure 1), which were naturally latent under ambient conditions because of the change in the complexes' geometries [17]. These complexes could promote several olefin metathesis reactions when activated by visible light (420 nm or blue LEDs). In a recent approach, plasmonic nanoparticles considerably improved the initiation of phosphite-containing ruthenium olefin metathesis latent precatalysts by irradiation with low-energy deep red or infrared light [18].

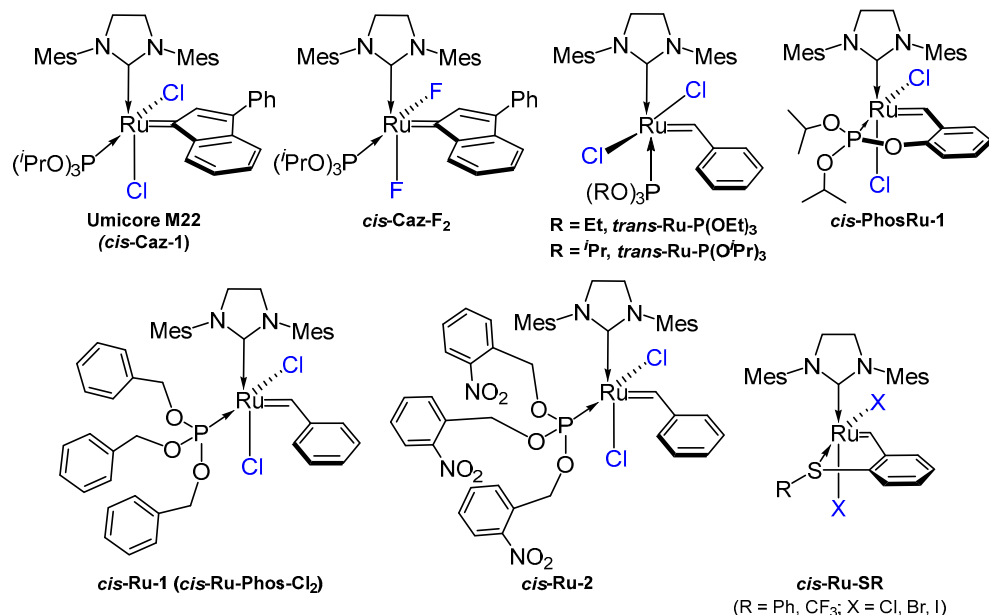


Figure 1. Selected ruthenium olefin metathesis catalysts containing phosphite- and sulfur-chelating indenylidene ligands.

The precise control of catalyst activity is a fundamental pursuit in the field of catalysis, with far-reaching implications for the development of efficient chemical processes and the synthesis of complex molecules. Anionic ligands serve as indispensable components in ruthenium olefin metathesis precatalysts, assuming multifaceted roles that profoundly influence catalytic behavior [19–27]. These ligands contribute to the stability of the ruthenium complex by coordinating to the metal center thereby mitigating decomposition and prolonging the catalyst's lifetime, especially in demanding or prolonged reactions. Further-

more, certain anionic ligands actively participate in the activation process of the precatalyst, facilitating the exchange of labile ligands with olefins or other substrates, a pivotal step in initiating metathesis reactions. Beyond this, they exert control over the reactivity of the catalyst, affecting reaction rates and even influencing regio- and stereoselectivity [21,22,28–30], permitting chemists to fine-tune catalytic performance for specific transformations. Additionally, anionic ligands can modulate the latency of the catalyst, enabling precise control over the timing of activation. Although exchanging chlorides with other anions many times resulted in decreased reactivity [19], in many other cases, significant novel applications, including improved stereo- and enantioselectivity [21,22,28–30], immobilization [23,24], water solubility [25], etc. could be achieved. Both bromides and iodides as anionic ligands are quite established in ruthenium complexes for metathesis reactions [27–36]. These halide ligands play crucial roles in fine-tuning the reactivity and properties of the ruthenium catalysts. Thus, by incorporating bromo or iodo ligands into the coordination sphere of the ruthenium center, the catalyst's behavior can be modified and even tuned. The choice of halide ligand can influence the catalyst's reactivity, stability, and ability to engage in metathesis reactions with specific substrates [28–30]. Additionally, halide ligands can easily undergo ligand exchange reactions, enabling the customization and optimization of the ruthenium complex's coordination environment for improved catalytic performance. This versatility makes bromo and iodo ligands valuable tools in the design and development of ruthenium-based catalysts. However, as Slugovc has previously shown, the full interchange of the chloride ligands in the Hoveyda–Grubbs 2nd generation catalyst (**HG-II-Cl**) is challenging [26]. On the other hand, *cis*-dichloro ruthenium precatalysts with sulfur-chelation facilitate the substitution of the anionic ligands by an enhanced *trans*-effect, offering a privileged pathway for halide exchange [27,33–37]. Overall, anionic ligands provide a versatile toolkit for the design and customization of ruthenium olefin metathesis precatalysts, enabling their application across a diverse spectrum of metathesis reactions in synthetic chemistry.

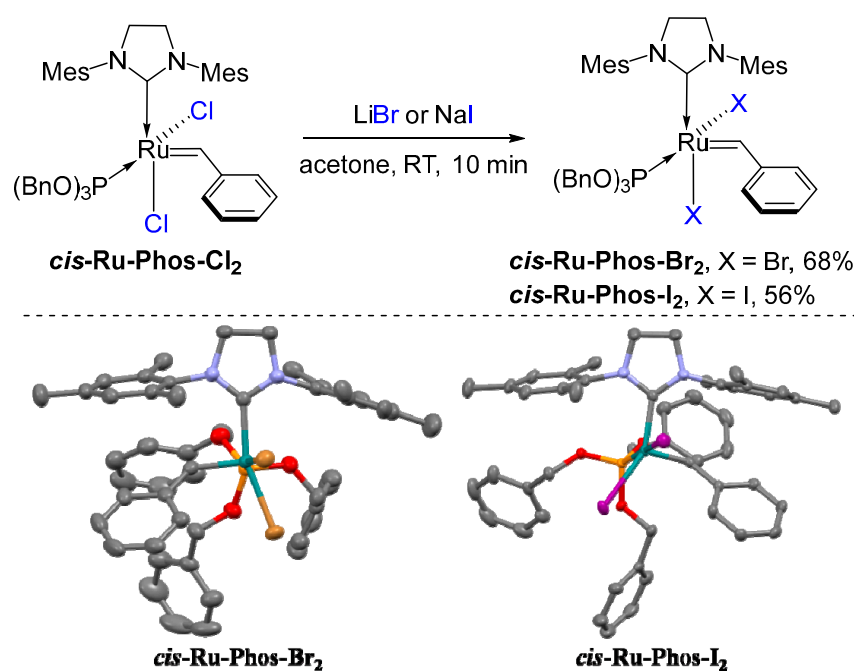
As previously mentioned, altering the anionic ligands in ruthenium alkylidenes can significantly alter the reactivity of these catalysts. Moreover, the selectivity of the catalysts towards different types of olefin metathesis reactions can also be altered. For example, making the anionic ligands larger prevents olefin metathesis of more sterically hindered double bonds, but can make reactions with terminal olefins more efficient (*vide infra*). Indeed, selectivity is a critical factor in controlling the stereochemistry of the newly formed double bonds. This is particularly valuable in the synthesis of complex organic molecules, such as natural products and pharmaceuticals, where the desired biological or chemical activity is often highly dependent on the stereochemical arrangement of the functional groups [4–8]. Regioselectivity is another facet of selectivity that guides olefin metathesis reactions to produce specific regioisomers when multiple products are possible, and these regioisomers may have different reactivities or biological activities. High selectivity is often associated with catalyst stability and longevity, which reduces the frequency of catalyst regeneration or replacement. Additionally, controlling the selectivity of the reactions aligns with the principles of green chemistry, as it reduces waste generation, minimizes the use of hazardous reagents, and conserves resources, making chemical processes more sustainable and environmentally friendly. The predictability afforded by selectivity in olefin metathesis reactions allows chemists to anticipate and control the outcomes of reactions, facilitating the design and optimization of synthetic routes. Selectivity is a cornerstone of efficient and sustainable chemical synthesis, offering benefits that span economic, environmental, and scientific domains.

Understanding the impact of anionic ligands is essential for the rational design and optimization of metathesis catalysts for various synthetic applications. In this context, the current work explores a pivotal aspect of catalyst modulation by investigating the tuning of latency through anionic ligand exchange in ruthenium benzyldiene phosphite complexes. Given the above, it may be of interest to study the influence of (bromo and iodo) anionic ligands on latent benzyldiene phosphite complexes. Herein, we show the

synthesis, characterization, and study of two new latent benzylidene phosphite ruthenium complexes with bromo and iodo anionic ligands and their activity in various metathesis reactions by thermal and photochemical activation.

2. Results and Discussion

Simple chlorides are remarkably common anionic ligands in the field of ruthenium alkylidenes. Chlorides serve as crucial ancillary ligands, stabilizing the ruthenium center and influencing its reactivity. They can modulate the electronic properties of the metal leading to variations in catalytic activity and selectivity. Nonetheless, other anions have been successfully implemented in several applications [27–36]. For example, iodide-containing ruthenium alkylidenes have shown outstanding efficiency in asymmetric olefin metathesis [28–30], unique reactivities, and unprecedented product selectivity [33]. Thus, we became interested in studying the bromo and iodo derivatives of latent benzylidene phosphite precatalysts (Scheme 1). These substitutions may provide more control by allowing for the fine-tuning of reactivity by altering reaction kinetics. Additionally, bromo and iodo halogen ligands can change the selectivity of metathesis processes, affecting stereoselectivity and regioselectivity.



Scheme 1. Synthesis by anionic ligand exchange (top) and single crystal X-ray structures of *cis*-Ru-Phos-Br₂ and *cis*-Ru-Phos-I₂ complexes (bottom). Reaction conditions: *cis*-Ru-Phos-Cl₂ (50 mg), 10 eq. salt (LiBr or NaI), 1.5 mL acetone at RT. Ellipsoids are shown at a 50% probability level. Hydrogen atoms and solvent molecules were omitted for clarity. CCDC number for *cis*-Ru-Phos-Br₂: 2297786 and *cis*-Ru-Phos-I₂: 2297788.

Catalyst synthesis and characterization: Complexes *cis*-Ru-Phos-Br₂ and *cis*-Ru-Phos-I₂ were readily obtained by mixing LiBr/NaI salts with *cis*-Ru-Phos-Cl₂ in acetone at room temperature (Scheme 1, top), affording purple- and brown-colored solids, respectively. Interestingly, both reactions were completed in short time periods (10 min), and the chloride ligands were fully replaced by bromide or iodide ligands, as observed by NMR spectroscopy. As expected, the NMR spectra of Ru-Phos-Br₂ revealed its *cis*-dibromo configuration, showing the benzylidene signal at 15.22 ppm and ³¹P NMR signal at 130.18 ppm for the phosphite ligand (Figures S1–S3). The ¹H-NMR spectrum for the *cis*-Ru-Phos-I₂ complex (Figure S4) showed the dynamic broadening of the signals. A sharp spectrum could be obtained by cooling to −8 °C, and readily disclosed the *cis*-diiodo configuration with the

benzylidene signal at 15.12 ppm and the ^{31}P NMR signal at 129.93 ppm (Figures S4–S7). For both complexes, slow pentane diffusion into a DCM solution at $-20\text{ }^{\circ}\text{C}$ produced suitable crystals for X-ray diffraction (Scheme 1, bottom).

Table 1 compares the differences in key bond lengths between the different *cis*-Ru-Phos- X_2 complexes. Notably, the Ru–P bond has similar bond lengths in all three complexes, while the Ru–NHC bond is peculiarly slightly shorter for the diiodo complex. On the other hand, the Ru–C_{benzylidene} bond length increased with increasing halogen ligand size, from 1.818 Å for the dichloro complex to 1.861 Å for the diiodo complex. Overall, all complexes had comparable structural arrangements; however, the nature of the anionic ligands has a certain influence on some bond lengths, which may have a noteworthy effect on the initiation rate, reaction propagation, and stability.

Table 1. Selected bond lengths of *cis*-Ru-Phos- X_2 complexes.

Bond Lengths (Å)	<i>cis</i> -Ru-Phos-Cl ₂	<i>cis</i> -Ru-Phos-Br ₂	<i>cis</i> -Ru-Phos-I ₂
Ru–P	2.256 (3)	2.226 (10)	2.250 (8)
Ru–NHC	2.067 (8)	2.067 (3)	2.043 (3)
Ru–C _{benzylidene}	1.818 (6)	1.844 (3)	1.861 (3)
Ru–X ₁ (trans to NHC)	2.404 (2)	2.535 (4)	2.720 (3)
Ru–X ₂ (trans to P)	2.401 (3)	2.565 (5)	2.741 (3)

Photochemical and thermal activation of *cis*-Ru-Phos- X_2 complexes: The relative activity of the halide complexes was then compared. As expected, *cis*-Ru-Phos-Br₂ is completely latent at room temperature for ring-closing metathesis (RCM) reactions. However, the *cis*-Ru-Phos-I₂ complex showed some RCM activity at room temperature, i.e., a reaction of diethyl diallylmalonate (DEDAM) with a 1 mol% catalyst in toluene- d_8 produced 41% conversion over the course of a 24 h reaction period. The enhanced activity of *cis*-Ru-Phos-I₂ at room temperature might be due to the longer bond lengths observed for the Ru–C_{benzylidene} bond. After assessing the latency for the new complexes, the photoactivation behavior was studied by irradiating toluene- d_8 solutions of the complexes with different wavelengths of light at ambient temperatures in the presence of DEDAM (Figure 2).

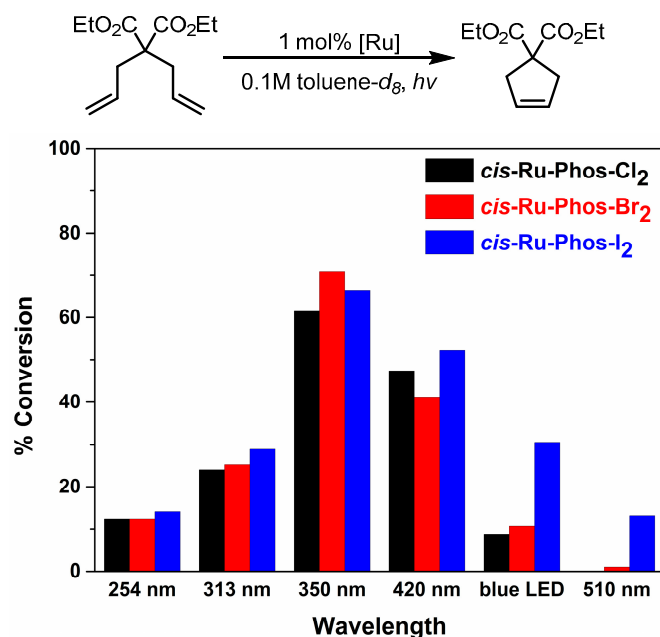


Figure 2. Photochemical activation of *cis*-Ru-Phos- X_2 complexes for the RCM reaction of DEDAM at different wavelengths. Reaction conditions: 1 mol% catalyst, 0.1 M toluene- d_8 , 2 h. Conversions were monitored and determined by ^1H NMR.

Surprisingly, the anionic ligands do not have a significant effect on the observed photoinduced activity (Figure 2). In general, 350 nm (UV-A) and 420 nm produced the most efficient results. Given the results observed in the photoinduced RCM of DEDAM, a larger scope of RCM substrates was probed, affording good to excellent conversions when the catalysts were activated by UVA irradiation (Table 2). Under photochemical activation with *cis*-Ru-Phos-Cl₂ and *cis*-Ru-Phos-Br₂, the reactions with hindered substrates that form trisubstituted olefins worked reasonably well (Table 2, entries 5 and 6); on the contrary, poor results were obtained with *cis*-Ru-Phos-I₂.

Table 2. Thermal and photochemical activation of complexes.

Entry	Substrates	Catalyst (1 mol%)	Thermal (80 °C) % conv. ^a	Photochemical(350 nm) % conv. ^b
1		<i>cis</i> -Ru-Phos-Cl ₂	4	62
		<i>cis</i> -Ru-Phos-Br ₂	16	71
		<i>cis</i> -Ru-Phos-I ₂	99	66
2		<i>cis</i> -Ru-Phos-Cl ₂	5	57
		<i>cis</i> -Ru-Phos-Br ₂	33	93
		<i>cis</i> -Ru-Phos-I ₂	99	93
3		<i>cis</i> -Ru-Phos-Cl ₂	15	92
		<i>cis</i> -Ru-Phos-Br ₂	20	99
		<i>cis</i> -Ru-Phos-I ₂	99	99
4		<i>cis</i> -Ru-Phos-Cl ₂	17	70
		<i>cis</i> -Ru-Phos-Br ₂	30	80
		<i>cis</i> -Ru-Phos-I ₂	97	81
5		<i>cis</i> -Ru-Phos-Cl ₂	29	80
		<i>cis</i> -Ru-Phos-Br ₂	42	78
		<i>cis</i> -Ru-Phos-I ₂	88	23
6		<i>cis</i> -Ru-Phos-Cl ₂	17	41
		<i>cis</i> -Ru-Phos-Br ₂	42	64
		<i>cis</i> -Ru-Phos-I ₂	99	29

^a Reaction conditions: 1 mol% catalyst, 0.1 M toluene-*d*₈, 80 °C, 10 min. ^b Reaction conditions: 1 mol% catalyst, 0.1 M toluene-*d*₈, 350 nm, 2 h. Conversions were monitored and determined by ¹H NMR (see Supporting Information).

In addition to the photochemical activation behavior, thermal activation was also studied. To highlight the differences between the different complexes, short reaction heating times (10 min) and relatively low temperatures (80 °C) were used. In contrast to the photoinduced reactions, thermal activation produced a clear trend with the different anionic ligands. Thus, *cis*-Ru-Phos-I₂ was much more efficient for all thermally activated reactions. Even RCM affording trisubstituted olefins showed quantitative conversion within less than 10 min. The thermally activated *cis*-Ru-Phos-Br₂ complex gave RCM results between the iodo and chloro homologues. Thus, while the results shown in Table 2 support the notion that thermally induced phosphite ligand dissociation is accelerated by the size of the anionic ligand (in this halide series), the photochemical dissociation is nearly oblivious to this trend.

Kinetic profile study: A kinetic profile study in olefin metathesis reactions involves the systematic investigation of the reaction's progress over time to understand its reaction mechanism, reaction rates, and factors that influence the reaction's kinetics. The kinetic

profiles for thermally induced RCM of di-, tri-, and tetra-substituted olefins were carefully followed to obtain further insights into the factors affecting the reactivity of these catalysts. With the exception of tetra-substituted olefins, the *cis*-Ru-Phos-I₂ was shown to be a much more effective catalyst than the others, supporting the results already shown in Table 2. The stark difference in activity can be observed in the RCM reaction of benchmark substrate diethyl diallylmalonate (DEDAM). While complete RCM is observed by using *cis*-Ru-Phos-I₂ in less than five minutes, *cis*-Ru-Phos-Br₂ and *cis*-Ru-Phos-Cl₂ provided less than 40% and 10% conversions, respectively (Figure 3). A similar trend was observed with diethyl 2-allyl-2-(2-methylallyl)-malonate as the RCM substrate (which provides a trisubstituted ring-closed product) (Figure 4). In sharp contrast, when 4-methyl-*N,N*-bis(2-methylallyl) benzene sulfonamide was used (and the catalyst loading increased), the diiodo catalyst could not promote any RCM, poor results were obtained with the dichloro catalyst, and better (but still sluggish) results were seen with the dibromo catalyst which notably proved to be the best for this kind of substrates (Figure 5). In any case, it seems that the higher steric hindrance exerted by the iodide ligands prevents ring-closing to tetra-substituted olefins. The reluctance of *cis*-Ru-Phos-I₂ to ring-close hindered olefins, coupled with the superb results seen with the less hindered substrates, may give rise to unique selectivities for specialized methodologies when using this latent catalyst. Additionally, *cis*-Ru-Phos-Br₂ remains fully latent at room temperature and has outstanding photochemical and thermal reactivity for a wide gamut of RCM substrates.

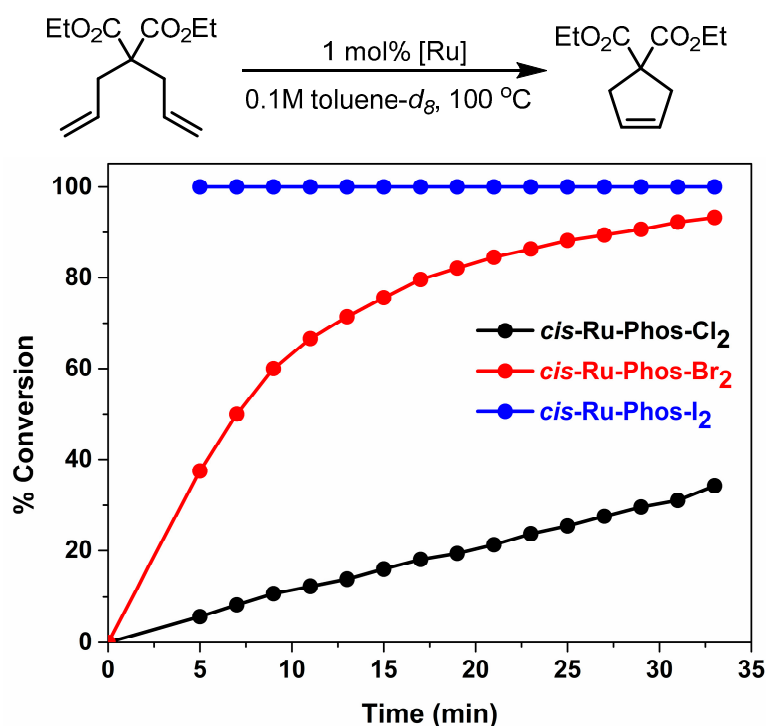


Figure 3. Kinetic profile of RCM reaction with DEDAM; toluene-*d*₈, 0.1 M, 100 °C, 1 mol% catalyst. Conversions were monitored and determined by ¹H NMR (see Supporting Information).

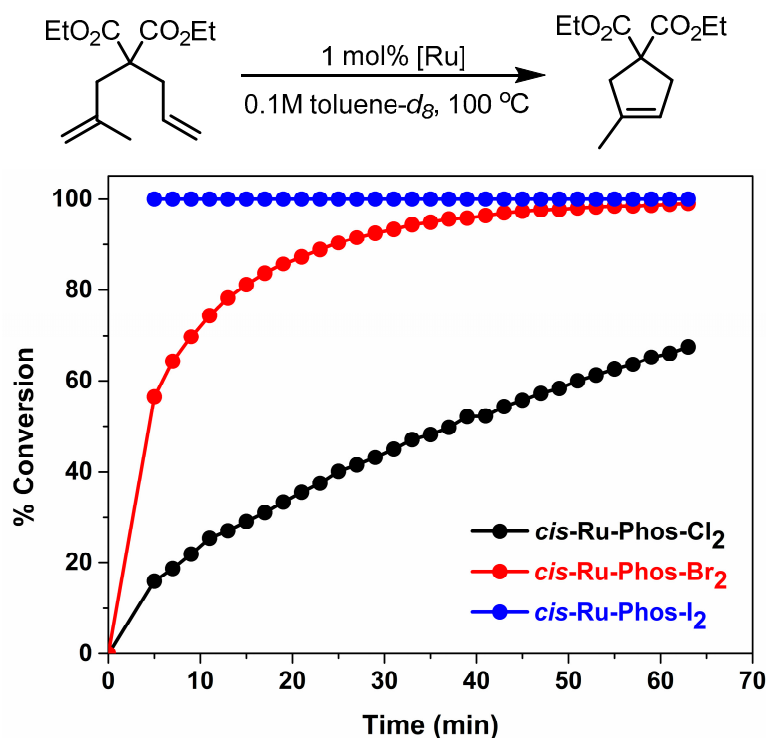


Figure 4. Kinetic profile of RCM reaction with diethyl 2-allyl-2-(2-methylallyl)-malonate; toluene- d_8 , 0.1 M, 100 °C, 1 mol% catalyst. Conversions were monitored and determined by ^1H NMR (see Supporting Information).

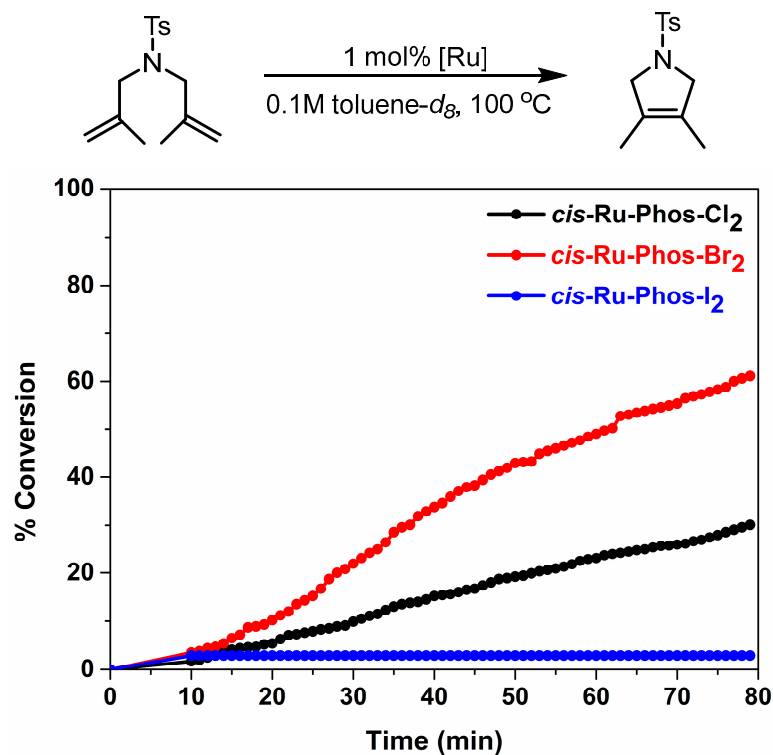


Figure 5. Kinetic profile of RCM reaction with 4-methyl-*N,N*-bis(2-methylallyl) benzene sulfonamide; toluene- d_8 , 0.1 M, 100 °C, 4 mol% catalyst. Conversions were monitored and determined by ^1H NMR (see Supporting Information).

Ring-opening metathesis polymerization (ROMP): Latent catalysts provide better control over the timing and extent of the polymerization reaction. This control allows for the synthesis of polymers with precise properties, such as molecular weight and dispersity. Since they are inactive until triggered, the risk of unintended polymerization or premature initiation is reduced. This is particularly important in industrial-scale polymerization processes where safety measures are paramount. The developments in ruthenium-based latent catalysts have played a significant role in the development and application of ROMP for the synthesis of advanced polymers and materials. Their ability to provide control over polymerization processes and their compatibility with a variety of monomers make them valuable tools in the field of polymer chemistry [38–40]. Here, we set out to investigate the potential for achieving carbon–carbon double bond selectivity in ROMP polymers by using our newly developed phosphite-containing catalysts. Curiously, thermal-activated ROMP was slow and afforded less than 50% conversion with 0.2 mol% catalyst loading in $C_2D_2Cl_4$ at 80 °C after 24 h. However, (and perhaps because of the low conversion) the polymers obtained by heating had an unusually high Z ratio of double bonds (Figure 4). When the same reactions were conducted under irradiation with 350 nm light with *cis*-Ru-Phos-Cl₂ and *cis*-Ru-Phos-Br₂, the reactions readily proceeded to full conversions with a greater *trans* double bond content in the polymer (Figure 6). Photoinduced ROMP with *cis*-Ru-Phos-I₂ was not very efficient and also gave high Z-content, as observed for the thermally induced polymerizations.

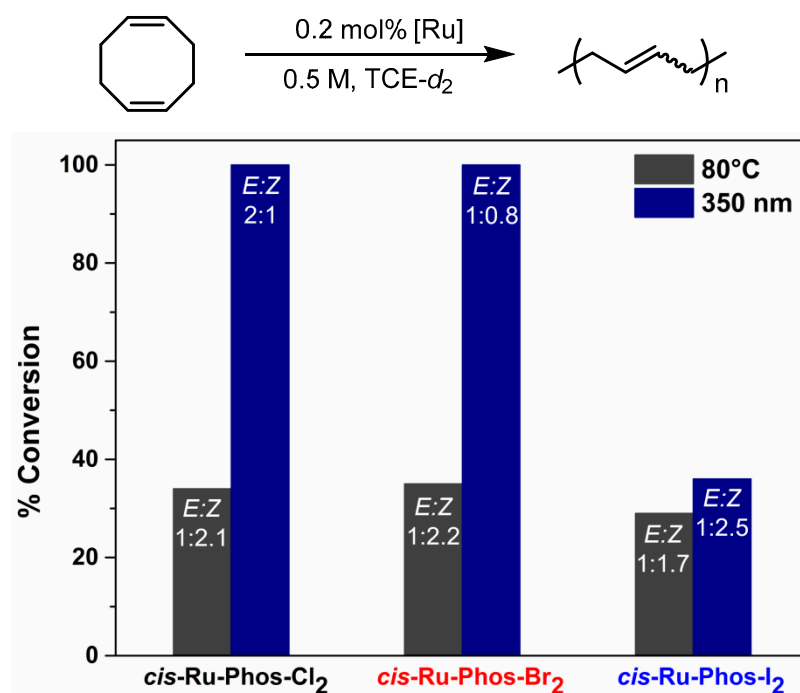


Figure 6. ROMP of COD, all conversions were determined by ¹H NMR using mesitylene as an internal standard. Conversions were monitored and determined by ¹H NMR (see Supporting Information).

3. Experimental Section

3.1. General

All commercially available solvents and reagents were of reagent grade and used without further purification unless otherwise stated. Purification by column chromatography was performed on Fluka silica gel 60 (40–60 μm). TLC analyses were performed using Merck pre-coated silica gel (0.2 mm) aluminum sheets. All nuclear magnetic resonance (NMR) spectra were acquired on Bruker DPX 400 or DPX 500 instruments (Bruker, Billerica, MA, USA); chemical shifts, given in ppm, are relative to Me₄Si as the internal standard or the residual solvent peak. HRMS analyses were done on a Q Exactive™ Focus by ThermoFisher

(Waltham, MA, USA) with an ESI probe. Irradiation experiments were carried out using a Luzchem Research LZC-ORG photoreactor (Luzchem Research, Ottawa, ON, Canada) and were carried out in 5 mm NMR tubes at room temperature. X-ray experimental data: Single crystals of *cis*-Ru-Phos-Br₂ and *cis*-Ru-Phos-I₂ were obtained by slow diffusion of pentane into dichloromethane solution of the complexes, respectively, at 5 °C.

3.2. Synthetic Procedure and Data for the Complexes

Synthesis of *cis*-Ru-Phos-Cl₂: It was done as previously reported [15].

Synthesis of *cis*-Ru-Phos-Br₂: A solution of lithium bromide (47.2 mg, 0.54 mmol, 5.0 equiv) in dry acetone (1 mL) was added to *cis*-Ru-Phos-Cl₂ (50.0 mg, 0.054 mmol, 1.0 equiv) in acetone (1.5 mL). The reaction mixture was stirred for 10 min and the color turned bright purple. The solvent was removed under vacuum; the crude was filtered over celite with DCM as an eluent. Solvents were removed under vacuum. A minimal amount of acetone was added, followed by the addition of hexane to obtain a purple solid. Filtration over Büchner and washing with hexane produced a dark purple solid (37.3 mg, 0.37 μmol, 68%). Crystals suitable for X-ray diffraction were obtained by slow diffusion of pentane to a DCM solution at −20 °C. ¹H NMR (DCM-*d*₂, 400 MHz): δ 15.22 (d, *J* = 24.0 Hz, 1H), 7.86 (d, 2H), 7.56 (t, 1H), 7.28–7.22 (m, 11H), 7.10–7.08 (m, 6H), 6.96 (s, 1H), 6.80 (s, 1H), 6.73 (s, 1H), 6.23 (s, 1H), 4.59–4.52 (m, 4H), 4.29–4.25 (m, 4H), 3.98–3.69 (m, 6H), 2.67 (s, 3H), 2.63 (s, 3H), 2.15 (s, 6H), 2.13 (s, 3H), 2.07 (s, 3H) ppm. ¹³C NMR (DCM-*d*₂, 125 MHz): δ 303.7, 208.0, 149.2, 138.8, 138.4, 138.2, 138.1, 137.4, 137.1, 135.5, 134.9, 131.9, 130.8, 130.1, 129.9, 129.7, 128.6, 128.2, 127.9, 127.3, 67.7, 51.8, 51.5, 21.8, 20.7, 20.6, 20.2, 19.1, 18.1 ppm. ³¹P NMR (DCM-*d*₂, 202 MHz): δ 130.18 ppm. HRMS *m/z*: calcd for [C₄₉H₃₅BrN₂O₃PRu]⁺, 929.2015; found, 931.2014.

Synthesis of *cis*-Ru-Phos-I₂: A solution of sodium iodide (81.4 mg, 0.54 mmol, 5.0 equiv) in dry acetone (1 mL) was added to *cis*-Ru-Phos-Cl₂ (50.0 mg, 0.054 mmol, 1.0 equiv) in acetone (1.5 mL). The reaction mixture was stirred for 10 min and the color turned dark brown. The solvent was removed under vacuum; the crude was filtered over celite with DCM as an eluent. Solvents were removed under vacuum. A minimal amount of acetone was added, followed by the addition of hexane to obtain a brown solid. Filtration over Büchner and washing with hexane produced a dark brown solid (33.5 mg, 0.30 μmol, 56%). Crystals suitable for X-ray diffraction were obtained by slow diffusion of pentane to a DCM solution at −20 °C. ¹H NMR (DCM-*d*₂, 500 MHz): δ 15.09 (d, *J* = 24.0 Hz, 1H), 7.91 (d, 2H), 7.61 (t, 1H), 7.28 (m, 9H), 7.21–7.07 (m, 8H), 6.93 (s, 1H), 6.77 (s, 2H), 6.33 (s, 1H), 6.23 (s, 1H), 4.54–4.49 (m, 4H), 4.28–4.25 (m, 4H), 3.95–3.81 (m, 6H), 2.69 (s, 3H), 2.62 (s, 3H), 2.22 (s, 3H), 2.18–2.14 (m, 9H) ppm. ¹³C NMR (DCM-*d*₂, 125 MHz): δ 302.0, 208.9, 149.6, 140.9, 138.8, 138.5, 138.1, 137.6, 136.8, 135.2, 134.6, 132.2, 130.4, 130.2, 129.7, 128.8, 128.4, 128.0, 127.9, 127.2, 67.3, 52.1, 51.9, 24.1, 22.6, 21.0, 20.8, 20.7, 19.5 ppm. ³¹P NMR (DCM-*d*₂, 202 MHz): δ 129.76 ppm. HRMS *m/z*: calcd for [C₄₉H₃₅IN₂O₃PRu]⁺, 977.1877; found, 977.1890.

3.3. General Procedures for Ring-Closing Metathesis (RCM)

An NMR tube was charged with a solution of substrates (diene) and a 1 mol% catalyst in toluene-*d*₈ (0.5 mL, 0.1 M). The reaction mixture was degassed with argon and then placed in an oil bath set at 80 °C for the specified period of time (thermal activation) and likewise placed inside the Luzchem LZC-ORG photoreactor for irradiation with 350 nm lamps for the specified period of time (photochemical activation). All conversions were determined by ¹H NMR.

3.4. General Procedures for Ring-Opening Metathesis Polymerization (ROMP)

An NMR tube was charged with a solution of 1,5-cyclooctadiene (COD) and a 0.2 mol% catalyst in 1,1,2,2-tetrachloroethane-*d*₂ (TCE-*d*₂) (0.5 mL, 0.5 M). The reaction mixture was degassed with argon and then placed in an oil bath set at 80 °C for the specified period of time (thermal activation) and placed inside the Luzchem LZC-ORG photoreactor for

irradiation with 350 nm lamps for the specified period of time (photochemical activation). All conversions and *E/Z* ratios in polymers were determined by ^1H NMR using mesitylene as an internal standard.

4. Conclusions

In summary, the work presented in this paper sheds light on the intricate relationship between anionic ligand exchange and latency control in ruthenium benzylidene phosphite complexes. To better understand the effects of halogen anionic ligand exchange on the family of latent ruthenium benzylidene phosphite complexes, *cis-Ru-Phos-Br₂* and *cis-Ru-Phos-I₂* were synthesized and studied. Both benzylidene complexes adopted the *cis*-dihalo configuration; *cis-Ru-Phos-Br₂* was found to be fully latent, while *cis-Ru-Phos-I₂* showed very low activity at ambient temperatures. The thermal and photochemical activation of these precatalysts for several olefin metathesis reactions was studied and compared with their chloride homologue. As expected, these new complexes were readily activated by light or heat, promoting a number of reactions (including RCM and ROMP), successfully expanding the toolkit for latent and photoinduced olefin metathesis. Significantly, *cis-Ru-Phos-I₂* displayed privileged initiation for RCM reactions of unhindered olefins. Overall, this study broadens the practical applicability for latent olefin metathesis reactions and improves the scientific knowledge of the concepts guiding thermal and photochemical activation as well as the rate of initiations for various halo anionic ligands in the latent ruthenium benzylidene family.

Supplementary Materials: The following supporting information can be downloaded at <https://www.mdpi.com/article/10.3390/catal13111411/s1>. The Supplementary Data contains the copies of NMR and HRMS spectra for complexes—Figures S1–S7; X-ray crystallographic data and structure refinement details—Table S1; copies of NMR data for the RCM reactions under thermal and photochemical conditions using different substrates—Figures S8–S61; NMR data for kinetic profile study with different substrates—Figures S62–S70; NMR data for ROMP study with COD under thermal and photochemical conditions—Figures S71–S76.

Author Contributions: Conceptualization, N.A., R.S.P. and N.G.L.; synthesis, characterization and experiments, N.A. and R.S.P.; writing—original draft preparation, N.A. and R.S.P.; solving the crystal structure of *cis-Ru-Phos-Br₂*, M.B.; writing—review and editing, all authors; supervision, O.R., R.S.P. and N.G.L.; funding acquisition, N.G.L. and O.R. All authors have read and agreed to the published version of the manuscript.

Funding: This work was supported by the grants of the Israel Science Foundation (ISF grant no. 506/18) and the Israel Innovation Authority (grant no. 76763).

Data Availability Statement: The data presented in this study are available in supplementary materials.

Acknowledgments: We are grateful to Natalia Fridman from the crystallographic lab at the Schulich Faculty of Chemistry, Technion, for contributing to the X-ray crystallographic study of *cis-Ru-Phos-I₂* (CCDC 2297788).

Conflicts of Interest: The authors declare no conflict of interest.

References

1. Hoveyda, A.H.; Zhugralin, A.R. The Remarkable Metal-catalysed Olefin Metathesis Reaction. *Nature* **2007**, *450*, 243–251. [[CrossRef](#)] [[PubMed](#)]
2. Grela, K. (Ed.) *Olefin Metathesis: Theory and Practice*; Wiley & Sons, Inc.: New York, NY, USA, 2014.
3. Grubbs, R.H.; Wenzel, A.G.; O’Leary, D.J.; Khosravi, E. (Eds.) *Handbook of Metathesis*; Wiley-VCH: Weinheim, Germany, 2015.
4. Nicolaou, K.C.; Bulger, P.G.; Sarlah, D. Metathesis Reactions in Total Synthesis. *Angew. Chem. Int. Ed.* **2005**, *44*, 4490–4527. [[CrossRef](#)]
5. Ogba, O.M.; Warner, N.C.; O’Leary, D.J.; Grubbs, R.H. Recent advances in ruthenium-based olefin metathesis. *Chem. Soc. Rev.* **2018**, *47*, 4510–4544. [[CrossRef](#)] [[PubMed](#)]
6. Higman, C.S.; Lummiss, J.A.M.; Fogg, D.E. Olefin Metathesis at the Dawn of Implementation in Pharmaceutical and Specialty-Chemicals Manufacturing. *Angew. Chem. Int. Ed.* **2016**, *55*, 3552–3565. [[CrossRef](#)] [[PubMed](#)]

7. Yu, M.; Lou, S.; Gonzalez-Bobes, F. Ring-Closing Metathesis in Pharmaceutical Development: Fundamentals, Applications and Future Directions. *Org. Process Res. Dev.* **2018**, *22*, 918–946. [[CrossRef](#)]
8. Tsedalu, A. A Review on Olefin Metathesis Reactions as a Green Method for the Synthesis of Organic Compounds. *J. Chem.* **2021**, *2021*, e3590613.
9. Liu, P.; Ai, C. Olefin Metathesis Reaction in Rubber Chemistry and Industry and Beyond. *Ind. Eng. Chem. Res.* **2018**, *57*, 3807–3820. [[CrossRef](#)]
10. Gladiali, S.; Alberico, E. Asymmetric transfer hydrogenation: Chiral ligands and applications. *Chem. Soc. Rev.* **2006**, *35*, 226–236. [[CrossRef](#)]
11. Gorin, D.J.; Sherry, B.D.; Toste, F.D. Ligand effects in homogeneous Au catalysis. *Chem. Rev.* **2008**, *108*, 3351–3378. [[CrossRef](#)]
12. Rogalski, S.; Pietraszuk, C. Application of Olefin Metathesis in the Synthesis of Carbo- and Heteroaromatic Compounds—Recent Advances. *Molecules* **2023**, *28*, 1680. [[CrossRef](#)]
13. Guidone, S.; Songis, O.; Nahra, F.; Cazin, C.S.J. Conducting Olefin Metathesis Reactions in Air: Breaking the Paradigm. *ACS Catal.* **2015**, *5*, 2697–2701. [[CrossRef](#)]
14. Antreil, X.; Schmid, T.E.; Randall, R.A.M.; Slawin, A.M.Z.; Cazin, C.S.J. Mixed *N*-heterocyclic carbene/phosphite ruthenium complexes: Towards a new generation of olefin metathesis catalysts. *Chem. Commun.* **2010**, *46*, 7115–7117. [[CrossRef](#)] [[PubMed](#)]
15. Eivgi, O.; Guidone, S.; Frenklah, A.; Kozuch, S.; Goldberg, I.; Lemcoff, N.G. Photoactivation of Ruthenium Phosphite Complexes for Olefin Metathesis. *ACS Catal.* **2018**, *8*, 6413–6418. [[CrossRef](#)]
16. Schmid, T.E.; Bantreil, X.; Citadelle, C.A.; Slawin, A.M.Z.; Cazin, C.S.J. Phosphites as ligands in ruthenium-benzylidene catalysts for olefin metathesis. *Chem. Commun.* **2011**, *47*, 7060–7062. [[CrossRef](#)]
17. Eivgi, O.; Vaisman, A.; Nechmad, N.B.; Baranov, M.; Lemcoff, N.G. Latent Ruthenium Benzylidene Phosphite Complexes for Visible Light Induced Olefin Metathesis. *ACS Catal.* **2020**, *10*, 2033–2038. [[CrossRef](#)]
18. Lemcoff, N.; Nechmad, N.B.; Eivgi, O.; Yehezkel, E.; Shelonchik, O.; Phatake, R.S.; Yesodi, D.; Vaisman, A.; Biswas, A.; Lemcoff, N.G.; et al. Plasmonic Visible–near Infrared Photothermal Activation of Olefin Metathesis Enabling Photoresponsive Materials. *Nat. Chem.* **2023**, *15*, 475–482. [[CrossRef](#)]
19. Albalawi, M.O.; Falivene, L.; Jedidi, A.; Osman, O.I.; Elroby, S.A.; Cavallo, L. Influence of the Anionic Ligands on Properties and Reactivity of Hoveyda-Grubbs Catalysts. *Mol. Catal.* **2021**, *509*, 111612.
20. Buchmeiser, M.R.; Anderson, E.B. Pseudo-halide Derivatives of Grubbs- and Schrock-Type Catalysts for Olefin Metathesis. *Synlett* **2012**, *2012*, 185–207. [[CrossRef](#)]
21. Engl, P.C.; Santiago, C.B.; Gordon, C.P.; Liao, W.; Fedorov, A.; Copéret, C.; Sigman, M.S.; Togni, A. Exploiting and Understanding the Selectivity of Ru-*N*-Heterocyclic Carbene Metathesis Catalysts for the Ethenolysis of Cyclic Olefins to α,ω -Dienes. *J. Am. Chem. Soc.* **2017**, *139*, 13117–13125. [[CrossRef](#)]
22. Khan, R.K.M.; Torke, S.; Hoveyda, A.H. Readily Accessible and Easily Modifiable Ru-Based Catalysts for Efficient and *Z*-Selective Ring-Opening Metathesis Polymerization and Ring-Opening/Cross-Metathesis. *J. Am. Chem. Soc.* **2013**, *135*, 10258–10261. [[CrossRef](#)]
23. Halbach, T.S.; Mix, S.; Fischer, D.; Maechling, S.; Krause, J.O.; Sievers, C.; Blechert, S.; Nuyken, O.; Buchmeiser, M.R. Novel Ruthenium-Based Metathesis Catalysts Containing Electron-Withdrawing Ligands: Synthesis, Immobilization, and Reactivity. *J. Org. Chem.* **2005**, *70*, 4687–4694. [[CrossRef](#)] [[PubMed](#)]
24. Braddock, D.C.; Tanak, K.; Chadwick, D.; Böhm, V.P.W.; Roeper, M. Vacuum-driven anionic ligand exchange in Buchmeiser-Hoveyda-Grubbs ruthenium(II) benzylidenes. *Tetrahedron Lett.* **2007**, *48*, 5301–5303. [[CrossRef](#)]
25. Gawin, R.; Czarnačka, P.; Grela, K. Ruthenium catalysts bearing chelating carboxylate ligands: Application to metathesis reactions in water. *Tetrahedron* **2010**, *66*, 1051–1056. [[CrossRef](#)]
26. Wappel, J.; Urbina-Blanco, C.A.; Abbas, M.; Albering, J.H.; Saf, R.; Nolan, S.P.; Slugovc, C. Halide exchanged Hoveyda-type complexes in olefin metathesis. *Beilstein J. Org. Chem.* **2010**, *6*, 1091–1098. [[CrossRef](#)] [[PubMed](#)]
27. Ivry, E.; Nechmad, N.B.; Baranov, M.; Goldberg, I.; Lemcoff, N.G. Influence of Anionic Ligand Exchange in Latent Sulfur-Chelated Ruthenium Precatalysts. *Inorg. Chem.* **2018**, *57*, 15592–15599. [[CrossRef](#)]
28. Seiders, T.J.; Ward, D.W.; Grubbs, R.H. Enantioselective Ruthenium-Catalyzed Ring-Closing Metathesis. *Org. Lett.* **2001**, *3*, 3225–3228. [[CrossRef](#)]
29. Gillingham, D.G.; Kataoka, O.; Garber, S.B.; Hoveyda, A.H. Efficient Enantioselective Synthesis of Functionalized Tetrahydropyrans by Ru-Catalyzed Asymmetric Ring-Opening Metathesis/Cross-Metathesis (AROM/CM). *J. Am. Chem. Soc.* **2004**, *126*, 12288–12290. [[CrossRef](#)]
30. Berlin, J.M.; Goldberg, S.D.; Grubbs, R.H. Highly Active Chiral Ruthenium Catalysts for Asymmetric Cross- and Ring-Opening Cross-Metathesis. *Angew. Chem. Int. Ed.* **2006**, *45*, 7591–7595. [[CrossRef](#)]
31. Dias, E.L.; Nguyen, S.T.; Grubbs, R.H. Well-Defined Ruthenium Olefin Metathesis Catalysts: Mechanism and Activity. *J. Am. Chem. Soc.* **1997**, *119*, 3887–3897. [[CrossRef](#)]
32. Sanford, M.S.; Love, J.A.; Grubbs, R.H. Mechanism and Activity of Ruthenium Olefin Metathesis Catalysts. *J. Am. Chem. Soc.* **2001**, *123*, 6543–6554. [[CrossRef](#)]
33. Nechmad, N.B.; Phatake, R.S.; Ivry, E.; Poater, A.; Lemcoff, N.G. Unprecedented Selectivity of Ruthenium Iodide Benzylidenes in Olefin Metathesis Reactions. *Angew. Chem. Int. Ed.* **2020**, *9*, 3539–3543. [[CrossRef](#)] [[PubMed](#)]

34. Bieszczad, B.; Barbasiewicz, M. The Key Role of the Nonchelating Conformation of the Benzylidene Ligand on the Formation and Initiation of Hoveyda–Grubbs Metathesis Catalysts. *Chem. Eur. J.* **2015**, *21*, 10322–10325. [[CrossRef](#)] [[PubMed](#)]
35. Phatake, R.S.; Nechmad, N.B.; Reany, O.; Lemcoff, N.G. Highly Substrate-Selective Macrocyclic Ring Closing Metathesis. *Adv. Synth. Cat.* **2022**, *364*, 1465–1472. [[CrossRef](#)]
36. Alassad, N.; Nechmad, N.B.; Phatake, R.S.; Reany, O.; Lemcoff, N.G. Steric and Electronic Effects in Latent S-Chelated Olefin Metathesis Catalysts. *Catal. Sci. Technol.* **2023**, *13*, 321–328. [[CrossRef](#)]
37. Grudzień, K.; Żukowska, K.; Malińska, M.; Woźniak, K.; Barbasiewicz, M. Mechanistic Studies of Hoveyda–Grubbs Metathesis Catalysts Bearing S-, Br-, I-, and N-coordinating Naphthalene Ligands. *Chem. Eur. J.* **2014**, *20*, 2819–2828. [[CrossRef](#)] [[PubMed](#)]
38. Weitekamp, R.A.; Atwater, H.A.; Grubbs, R.H. Photolithographic Olefin Metathesis Polymerization. *J. Am. Chem. Soc.* **2013**, *135*, 16817–16820. [[CrossRef](#)]
39. Nguyen, S.T.; Johnson, L.K.; Grubbs, R.H.; Ziller, J.W. Ring-opening metathesis polymerization (ROMP) of norbornene by a Group VIII carbene complex in protic media. *J. Am. Chem. Soc.* **1992**, *114*, 3974–3975. [[CrossRef](#)]
40. Chen, Y.; Abdellatif, M.M.; Nomura, K. Olefin metathesis polymerization: Some recent developments in the precise polymerizations for synthesis of advanced materials (by ROMP, ADMET). *Tetrahedron* **2018**, *74*, 619–643.

Disclaimer/Publisher’s Note: The statements, opinions and data contained in all publications are solely those of the individual author(s) and contributor(s) and not of MDPI and/or the editor(s). MDPI and/or the editor(s) disclaim responsibility for any injury to people or property resulting from any ideas, methods, instructions or products referred to in the content.